Anal. Bioanal. Electrochem., Vol. 11, No. 11, 2019, 1559-1574

Analytical & Bioanalytical Electrochemistry

www.abechem.com

Full Paper

Electrocatalytic Oxidation of Ethanol on Glassy Carbon Electrode Modified by Platinum Nanoparticles Dispersed into MMT/PANI/CS Composite Films

Masomeh Paydar,[1] Gholam Hossein Rounaghi,[1,*] Mohammd Hossein Arbab Zavvar,[1] Iman Razavipanah[1] and Parisa Mirhoseini Moosavi[2]

[1]*Department of Chemistry, Faculty of Sciences, Ferdowsi University of Mashhad, Mashhad, Iran*
[2]*Department of Soil Science, Faculty of agriculture, Ferdowsi University of Mashhad, Mashhad, Iran*

*Corresponding Author, Tel.: +985137626388; Fax: +985138796416
E-Mail: ghrounaghi@yahoo.com, ronaghi@um.ac.ir

Received: 16 August 2019 / Received in revised form: 5 November 2019 / Accepted: 6 November 2019 / Published online: 30 November 2019

Abstract- In this research work, montmorillonite/polyaniline/chitosan/platinum (MMT/PANI/CS/Pt) nanocomposite is used as an effective and novel catalyst for electrooxidation of ethanol. The glassy carbon electrode surface is coated with MMT/PANI and chitosan by applying a constant potential. Thereafter, the surface of the GCE is potentiostatically coated with platinum nanoparticles. The constructed electrode is referred to as: GCE/MMT/PANI/CS/Pt. The electrooxidation of ethanol molecules on the surface of MMT/PANI/CS/Pt electrode is studied using various electrochemical methods such as cyclic voltammetry, chronoamperometry and electrochemical impedance spectroscopy (EIS). The experimental results, indicate that the GCE/MMT/PANI/CS/Pt electrode possess a higher catalytic activity for ethanol electrooxidation compared to the GCE/Pt electrode. The Tafel plots indicate a better kinetic for ethanol electrooxidation in the presence of MMT/PANI/CS. The effect of various parameters on electrocatalytic oxidation of the ethanol molecules, such as the amount of platinum nanoparticles, MMT/PANI and ethanol concentration on the modified electrodes is investigated for electrooxidation of ethanol molecules using the GCE/MMT/PANI/CS/Pt electrode. The optimum conditions are obtained with 0.011 mg cm^{-2} Pt nanoparticle, 0.08 w/v% MMT/PANI and 1 M ethanol.

Keywords- Electrooxidition, Ethanol, Montmorillonite natural clay, PANI conducting polymer, Tafel study

1. INTRODUCTION

Due to the growing utilization of fossil fuels and the increasing environmental pollution, efficient and green energy is urgently needed. Recently, fuel cells have been receiving great number attention as they are clean energy conversion devices with environmentally green operations [1]. The direct alcohol fuel cells (DAFCs) is one of the most attractive ones due to their potential applications in transportation and portable electronic sources [2–4]. Particularly, direct ethanol fuel cells (DEFCs) are expected to be a promising one in the area of portable power sources and transportation due to the specific advantages of ethanol such as high power density, low toxicity, renewability and easy handling of liquid fuel [5–10]. The ethanol oxidation reaction mechanism at low temperatures, is limited due to the difficulty of C-C bond breaking and twelve electrons releasing processes. Thus, it is essential to accelerate this reaction by using of electrocatalyst [11].

To date, platinum is considered as the most effective and promising catalytic materials in DAFCs [12–14]. However, the platinum is too expensive. In addition, Pt is easily poisoned at its surface by the adsorption of reaction intermediates such as CO [15]. Alloying of the Pt with another metal, such as Sn, Ru, Ir, Rh, W, Mo and Os, is a convenient way to provide a higher catalytic performance of the electrodes for ethanol electrooxidation which are not cost effective [16–19]. Another way, is distributing the Pt metal into less expensive materials [20–23]. The use of a suitable supporting material, is an important factor which affects the performance of the supported electrocatalysts due to the interactions and surface reactivity [24]. Recently, attempts have been carried out to develop new supports by using of a polymer composite as Pt catalyst support for fuel cells [25–28]. To improve the catalytic activity of Pt nanoparticles, we synthesized a MMT/PANI/CS composite. Minerals natural clay can be used as catalyst supports in order to modify the surface of the electrodes for ethanol electrooxidation [29]. The natural clay is easily obtained and it is much less expensive than the costly metals. The immobilization of Pt nanoparticles on to the natural clay, reduces the Pt dosage. The clay layer is able to attract more Pt nanoparticles and significantly improves the surface area of the electrode [30]. MMT is a subgroup and common member of the smectite clay that is very effective as a catalyst from the synthetic organic chemist view point [31]. The MMT crystal structure is made up of an octahedral sheet of alumina and which between two tetrahedral sheets of silicon oxide [32]. The monovalent and divalent cations which often occupy the interlayer area in MMT, can be easily exchanged by the other ions which makes the MMT to be conductive and suitable catalyst support for modification of the fuel cells anode electrodes [33]. The hydrophilic MMT can be changed to an organophilic compound in order to make it miscible with the organic polymers via ion-exchange reaction [34]. On the other hand, many literatures have indicated that the conducting polymers (CPs) with a large surface area and high stability can be used to improve the dispersal of the metal particles [35,36]. The PANI, is an important and useful conducting polymer due to its stability and also simple and low cost of its

synthesis [37]. In addition, PANI can be considered as the most favorable matrix for dispersing the Pt nanoparticles because of its good adherence with the substrate of the electrode and also chemical stability [38]. In this study, a novel modified electrode was fabricated for ethanol electrooxidation based on MMT/PANI/CS composite and Pt nanoparticles. Montmorillonite natural clay and PANI conducting polymer as a material with a high surface area were used in order to enhance the ethanol electrooxidation efficiency.

2.EXPERIMENTAL

2.1. Material and reagents

All chemical reagents were of analytical grade. Aniline was purchased from Merck chemical company and it was purified by distillation and refrigerated until use. Perchloric acid, ethanol, ammonium persulfate, sulfuric acid, $H_2PtCl_6.6H_2O$ all purchased from Merck chemical company. A raw Na-bentonite sample, was collected from the mining site of Ghaen city in the South Khorasan province, Iran. All solutions were prepared with double distilled water.

2.2. Instrumentation

The electrochemical experiments were carried out at room temperature using a Potentiostat-Galvanostat (μ-Autolab Type III, ECO chemie) workstation which was equipped with an USB electrochemical interface and driven NOVA software. A conventional three-electrode cell was used in this study. The three-electrode cell, was consisted of an Ag/AgCl electrode (Azar Electrode Co., Urmia, Iran), a Pt wire electrode (Metrohm) and a glassy carbon electrode (Azar Electrode Co., Urmia, Iran) with a diameter of 2 mm. The structure of the montmorillonite was characterized by Philips PW 1800 X-ray diffraction (XRD) with Cu-K_α radiation (λ=1.54 Å). The surface morphology studies of the modified electrodes were performed by scanning electron microscopy (SEM, LEO 1450 VP). The Surface elemental analysis of the electrode was performed by energy dispersive X-ray technique using Oxford-7353 EDX microanalyzer. The morphology and structure of MMT/PANI, were characterized with transmission electron microscopy (TEM, LEO–912 AB). The electrochemical impedance spectroscopic measurements were carried out in the frequency range of 0.1 Hz to 30000 Hz with an amplitude of 10 mV with AC signals.

2.3. Synthesis of MMT/PANI composite

2.3.1. Preparation of MMT

The representative sample of the raw bentonite exhibited a mineral composition of mainly dioctahedral smectite and non-clay minerals such as quartz, feldspars, calcite, cristobalite, gypsum and mica. Quartz and feldspars are the main impurity phases. Theses impurities, often adversely affect the quality of the final product, therefore, the bentonite sample needs some processing to be free from the impurities. At the first stage, the purification process was performed by removing unwanted microorganisms and organic materials from samples using thermal processing at about 350°. The bentonite sample was subjected to the combination of purification methods which include wet sieving sedimentation, centrifugation and ultrasonification. The purification was carried out according to the method described in reference [39]. In order to separate the pure montmorillonite particles from (particle size-fractions required less than 2 μm) undesirable minerals (quartz, feldspar, etc.), 50 g of bentonite was dispersed in 1L of distilled water by laying the cylinder and it was stirred mechanically for several minutes. The sand fraction (>20 μm) was separated from the silt fraction using a 20 μm sieve. The residual of suspension, was allowed to stand for 24 h for separation of clay particles, then the clay suspension was stirred again and the clear supernatant liquid containing clay with the particles less than 2 μm, was collected after 4.5 h from a distance of 6.1 cm [40]. The supernatant liquid was siphoned into 100 mL centrifuge bottles and was collected by centrifugation at a certain speed for 5 min. The sedimentation and siphoning processes were repeated until very little clay particles were left in the suspension. Chemical treatments were applied for removing the impurities such as salts, gypsum and calcium carbonate from the samples [39]. Sodium acetate–acetic acid (pH 5) buffer solution was used to remove the carbonates from the samples [40]. At the final stage, the montmorillonite clay was obtained by cation exchange process with sodium chloride to produce homogeneous interlayer cations and the product was dried in an oven at 60 °C and then it was ground to a powder.

2.3.2. Preparation of MMT/PANI

For preparation of MMT/PANI, 0.6 ml of freshly distilled aniline was added to the 1 gr clay in glass tube and stirred for 15 minutes at room temperature. Then, 20 ml of sulfuric acid solution (0.2 M) was added to the mixture and the mixture was stirred for 30 min. Then, 20 ml ammonium persulfate solution (5 mM) was added drop wise to the resulting mixture and allowed to stir for 2.5 h. In the next step, the mixture was centrifuged at 10000 rpm and a green colored precipitate was formed at the bottom of the tube. The precipitate was rinsed several times with water - ethanol (1:1, $^{V}/_{V}$) mixture and dried for 3.5 h in a vacuum oven at 80 ℃ to obtain the MMT/PANI composite powder.

2.3.3. Preparation of GC/MMT/PANI/CS/Pt electrode

For construction of the modified electrode, a glassy carbon electrode (GCE) was polished with a slurry of 0.5 µm alumina and then rinsed with double distilled water. 0.04 g MMT/PANI composite and 0.015 g chitosan were added to 50 ml acetic acid (0.1 M) and sonicated for 15 minutes, until a homogeneous ink was formed. The MMT/PANI/CS mixture was electrochemically deposited at the surface of the GC electrode at a constant potential of -1.5 V for 300 s *vs.* Ag/AgCl reference electrode. The platinum nanoparticles were incorporated into the MMT/PANI/CS film by electrochemical deposition from an aqueous solution containing 2 mM $H_2PtCl_6.6H_2O$ and 0.2 M perchloric acid using a constant potential of -0.2 V *vs.* Ag/AgCl electrode. For comparison, the GC/Pt electrode was fabricated under the same experimental conditions, except the MMT/PANI/CS mixture was not electrochemically deposited at the surface of GC electrode.

3. RESULTS AND DISCUSSION

3.1. Structural characterization

3.1.1. X-ray diffraction analysis

The validation of the purification methods was determined based on X-ray, particle size, cation exchange capacity (CEC) and the ratio peak of the quartz/montmorillonite analysis pre and post experiments. X-ray diffraction (XRD) method was used for mineral phase analysis of the raw and the montmorillonite clay.

.

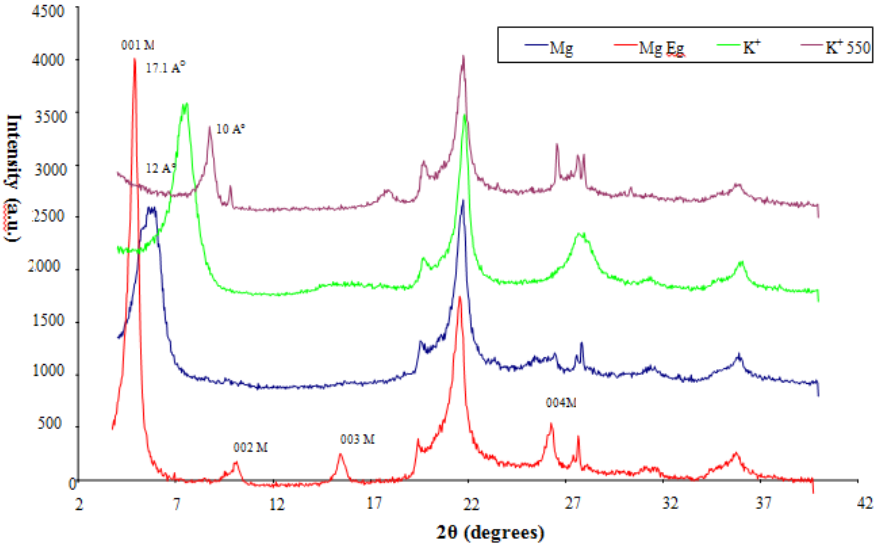

Fig. 1. XRD pattern of MMT

The XRD pattern was obtained from 2θ=4° to 60°. The XRD identification of the montmorillonite clay particles in clay fraction of the sample from the other minerals in smectite group, was carried out by routine test which involves Mg, Mg-glycerol, K^+ saturation and K^+ saturation at 550 °C treatments. The results are shown in Figure 1. As is evident in this Figure, the basal smectite peak is observed at 14 Å by applying the Mg saturation treatment. After saturation with Mg- glycol, the smectite peak shifts to 17.1 Å. After saturation with the K^+ ion, the smectite peak is observed at 12 Å which is collapsed to about 10 Å in K^+ saturation heating at 550 °C. These findings, indicate the presence of montmorillonite particles in less than 2 μm clay fraction. The particle size distribution of the purified montmorillonite clay, was determined by laser granulometry for determination the separation efficiency of the small particles from the whole materials using CORDOUAN model of particle size analyzer in Central Laboratory of Ferdowsi University of Mashhad, Iran.

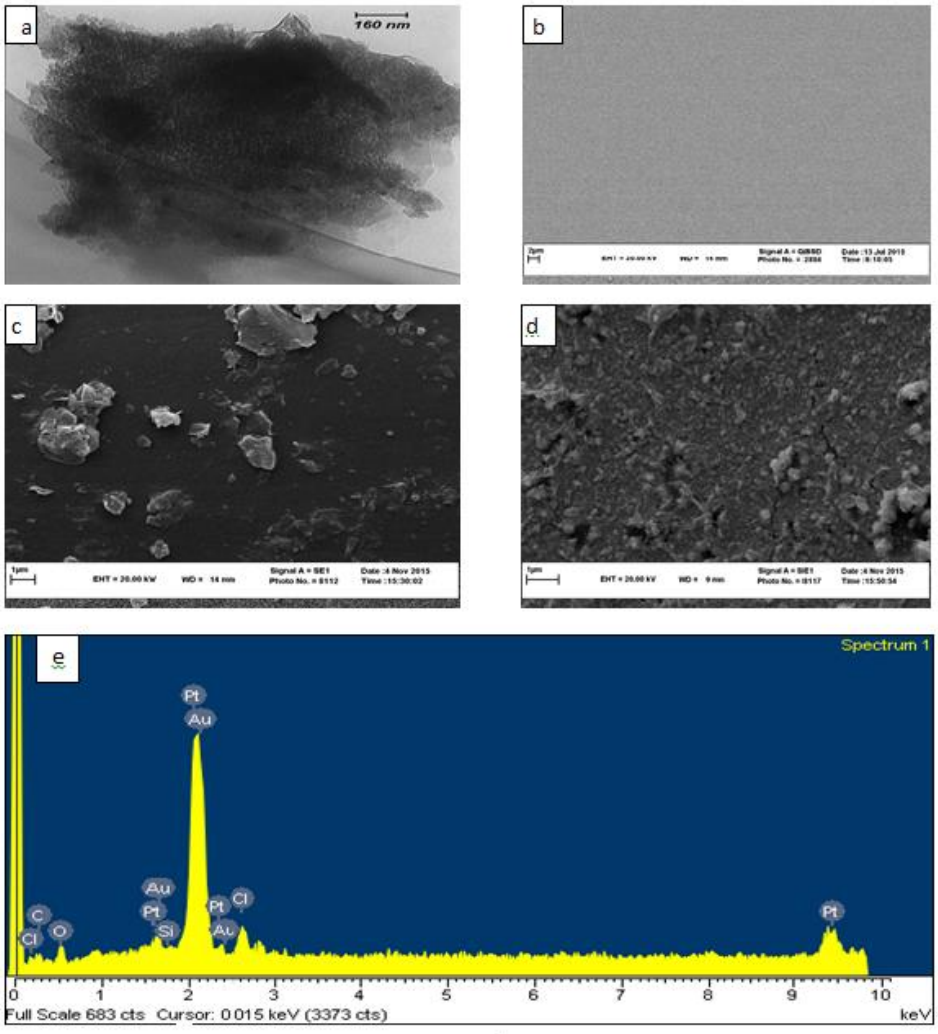

Fig. 2. (a) TEM image of MMT/PANI, (b) SEM image of bare GC, (c) SEM image of GC/MMT/PANI/CS, (d) GC/MMT/PANI/CS/Pt and (e) EDX spectrum of MMT/PANI/CS /Pt

3.1.2. TEM, SEM, and EDX characterization

The TEM image of the MMT/PANI composite is shown in Figure 2a. The formation of the dark polyaniline film on the surface of the MMT particle, can be observed from this TEM image. The micrograph of the bare GC, GC/MMT/PANI/CS and GC/MMT/PANI/CS/Pt electrodes has been investigated by SEM and the corresponding results are shown in Figures 2b, 2c and 2d respectively. Figure 2b, shows the surface of the bare glassy carbon electrode immediately after polishing with a slurry of 0.5 μm alumina. Inspection of Figure 2c, shows that the surface of the GCE is covered with the MMT/PANI/CS composite. Chitosan with high permeability toward water, good adhesion, biocompatibility and also nontoxicity, has been used to enhance the stability of MMT/PANI film on the surface of the constructed electrodes. The SEM micrograph of GC/MMT/PANI/CS modified with Pt nanoparticles is shown in Figure 2d. As in evident this Figure, the Pt nanoparticles are spread in a homogeneous arrangement on the surface of MMT/PANI/CS composite. For further evaluation of the immobilization of the MMT/PANI/CS composite on the surface the of GC electrode, EDX technique was also employed. The result is shown in Figure 2e. The existence of the essential peaks in this figure, clearly shows the formation of the novel MMT/PANI/CS/Pt electrocatalyst on the surface of the glassy carbon electrode.

3.2. Electrochemical characterizations of the modified electrode for ethanol electrooxidation

3.2.1. Cyclic voltammetry investigation

The electrocatalytic activity of the catalysts was estimated for ethanol electrooxidation by cyclic voltammetry technique. Figure 3 shows the cyclic voltammograms for electrooxidation of ethanol molecules, using the GC/Pt and GC/MMT/PANI/CS/Pt electrodes in 1 M solution of ethanol containing 0.3 M $HClO_4$ at scan rate 50 mVs^{-1}. As reported in the literature [41], three distinct oxidation peaks for ethanol oxidation are detected. Two oxidation peaks are appeared at 0.6 V (a) and 1.03 V (b) during positive potential scanning. In addition, in the reverse scan an anodic peak is observed at 0.36 V (c). The first oxidation peak (peak a) is ascribed to the formation of CO_2 [42], whereas the second oxidation peak (peak b) corresponds mainly to the formation of CH_3CHO molecules [41]. The anodic peak in the reverse scan (peak c) appears due to reoxidation of the ethanol and intermediate species (such as Pt–OCH_2CH_3, Pt–$CHOH–CH_3$, $(Pt)_2$ $COH–CH_3$, Pt–$COCH_3$ and Pt–CO) that are formed from incomplete oxidation of the ethanol molecules in the forward scan. These intermediates are oxidized hardly at low potentials which result in poison the electrocatalyst [11]. As can be seen in Figure 3, the GC/MMT/PANI/CS/Pt electrode shows a higher forward peak current density than the GC/Pt electrode. The high improvement in the catalytic activity of the proposed

electrode, is mainly attributes to the increasing the number of the catalytically active sites on the surface of GC/ MMT /PANI/CS/Pt electrode for electrooxidation of ethanol molecules.

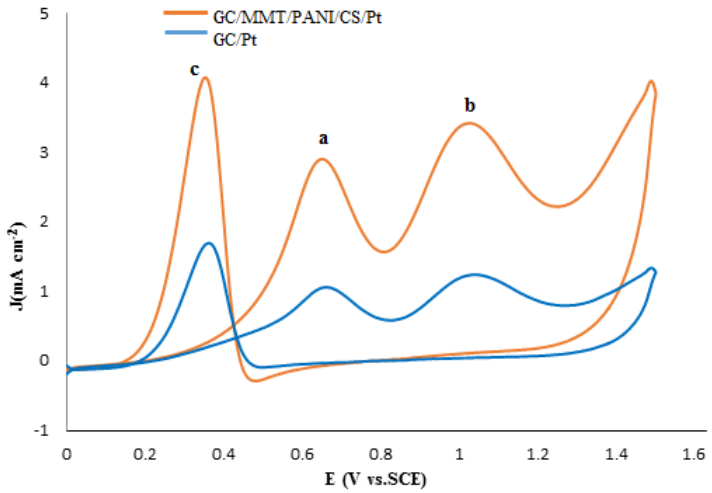

Fig. 3. Cyclic voltammograms of electrooxidation of ethanol using GC/Pt and GC/MMT/PANI/CS/Pt electrodes in 1M ethanol solution containing 0.3 M HClO4 at 50 mVs^{-1}

3.2.2. Electrochemical impedance spectroscopy

Electrochemical impedance spectroscopy (EIS) has been widely used as a powerful technique for studying the electron-transfer kinetics and examining the interfacial properties of the modified electrodes [43]. Figure 4A, shows the Nyquist plots of GC/Pt and GC/Clay/PANI/CS/Pt electrodes (*vs.* Ag/AgCl electrode) which are obtained in a solution containing 1 M of ethanol and 0.3M $HClO_4$. The equivalent circuit compatible with the results of the EIS investigations is presented in Figure 4B. In this circuit, R_s represents the solution resistance, CPE (constant-phase element) is the double-layer capacitance, and R_{ct} is the charge-transfer resistance [44]. A parallel combination of R_{ct} and CPE has been analyzed to form the semicircle, whose diameter has been considered as the ethanol oxidation transfer resistance. CPE can be obtained by the following equation [45]:

$$CPE= P^{1/n} R_{ct}^{1-n/n}$$

In this equation, P is the pre-factor of the CPE, and n is its exponent that represents the deviation of the element from the ideal behavior. Table 1, shows the values of the equivalent circuit elements which are obtained by fitting the experimental results. From the graphical results in Figure 4 and also the date in Table 1, it can be observed that the GC/MMT/PANI/CS/Pt electrode has lower charge transfer resistance values compared to the GC/Pt electrode. This behavior, indicates that the charge transfer process of ethanol electrooxidation occurring on the surface of GC/ MMT /PANI/CS/Pt electrode is faster than

that of the GC/Pt electrode. This enhancement can be due to homogenous dispersion of Pt nanoparticles on MMT/PANI/CS composite. Therefore, the MMT PANI/CS/Pt composite offers a most conductive surface for electrooxidation of ethanol molecules in $HClO_4$ solution.

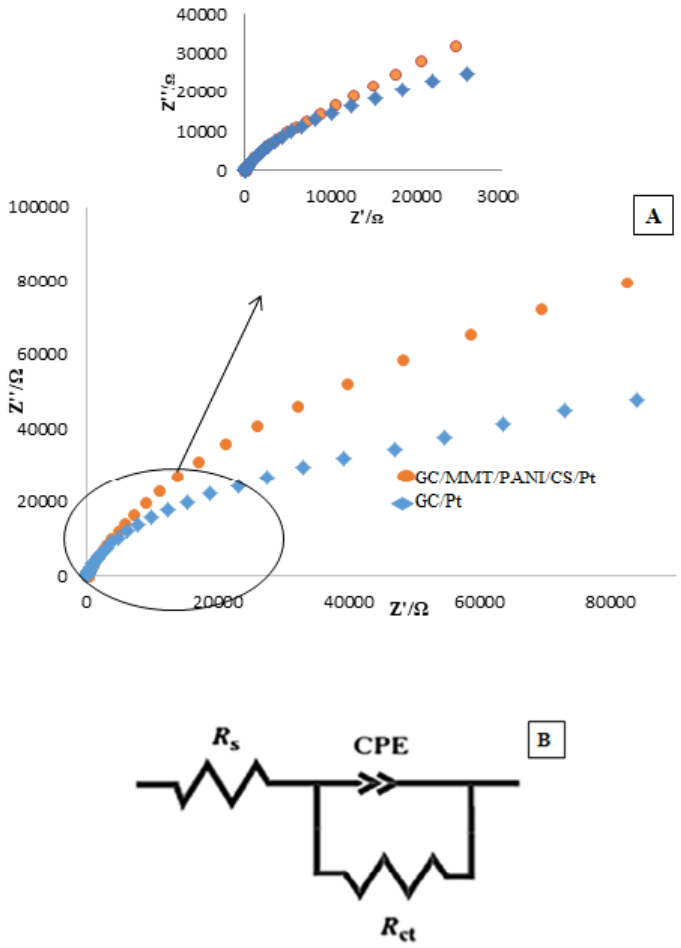

Fig. 4. (A) The Nyquist plots of GC/Pt and GC/MMT/PANI/CS/Pt electrodes (inset: high frequency region of Nyquist plots), (B) equivalent circuit

Table 1. The values of the elements in equivalent circuit fitted in the Nyquist plots of Fig. 4A

Electrode	R_1(Ohm)	R_2(Ohm)	P(pre exponential)	N(exponent)
GC/Pt	3.5	7534	0.00009	0.86
GC/MMT/PANI/CS/Pt	3.7	2581	0.00009	0.88

3.2.3. Chronoamperometric studies

The activity and the long-term performance of GC/MMT/PANI/CS/Pt and GC/Pt electrodes for ethanol electrooxidation are further considered by chronoamperometry

technique. Figure 5, displays the chronoamperometric curves for electrooxidation of ethanol molecules using the GC/Clay/PANI/C/Pt and GC/Pt electrodes in the 1 molar solution of ethanol at 0.93 V. This particular potential was chosen because it is close to the anodic peak potential in the cyclic voltammogram (see Figure 3). Both electrodes, show a continuous decay in the current density for electrooxidation of the ethanol molecules with time. The rapid decay of the current, could be related to the blocking of the surface of the electrodes with the CO_{ad} species. A more slowly decay of the current density with time implies that the catalyst acts as a good anti-poisoning agent. As can be seen in Figure 5, during the whole time of the experiment, the current density for the electrooxidation of ethanol molecules, in the case of GC/MM//PANI/CS/Pt electrode, is higher than that of the GC/Pt electrode. A careful inspection of this Figure, also confirms that the electrocatalytic activity of the GC/Clay/PANI/CS/Pt electrode is higher than the GC/Pt electrode due to the presence of the MMT/PANI/CS composite on the surface of the fabrication electrode.

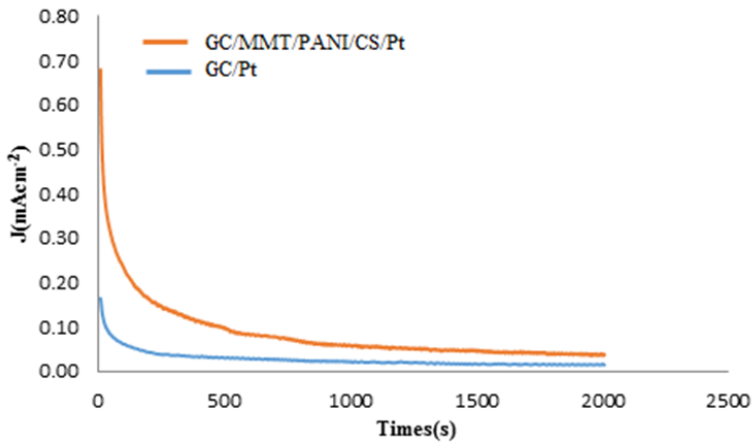

Fig. 5. Chronoamperometric curves of ethanol oxidation at GC/MMT/PANI/CS/Pt and GC/Pt electrodes, at a constant potential of 0.93 V *vs.* Ag/AgCl and at room temperature

3.3. Electrochemically active surface area

The cyclic voltammograms (CVs) of GC/Pt and the GC/MMT/PANI/CS/Pt catalysts in 0.3 mol L^{-1} $HClO_4$ solution are shown in Figure 6. The value of electrochemical active surface area (ECSA) can provide valuable information about the amount of electrochemically active sites and it can used for comparison of different electrocatalytic support. We can calculate the ECSA of GC/Pt and GC/MMT/PANI/CS/Pt electrodes by the following equation [46]:

$$ECSA=Q_H /[Q_0 \times Pt]$$

where Q_H (mC cm^{-2}) is the charge consumed during the electrodeposition of hydrogen on Pt surface at the potential range of -0.308 to 0.15 V (*vs.* Ag/AgCl electrode), the value of Q_0 which

is 0.21, represents the charge (mC cm^{-2}) which is required for oxidization a monolayer of hydrogen on the Pt surface and Pt, is the platinum loading on the electrode surface. Table 2, shows the physical characteristics of these two constructed electrodes. As evident in this Table, the ECSA of the GC/MMT/PANI/CS/Pt modified electrode is 1.3 times higher than that of GC/Pt electrode. Therefore, the modified electrode which has a higher accessible surface area, provides more active sites for electrooxidation of the ethanol molecules than GC/Pt electrode. Based on these experimental results, the MMT/PANI/CS composite has a positive effect in the electrode performance for electrooxidation of the ethanol molecules in solutions.

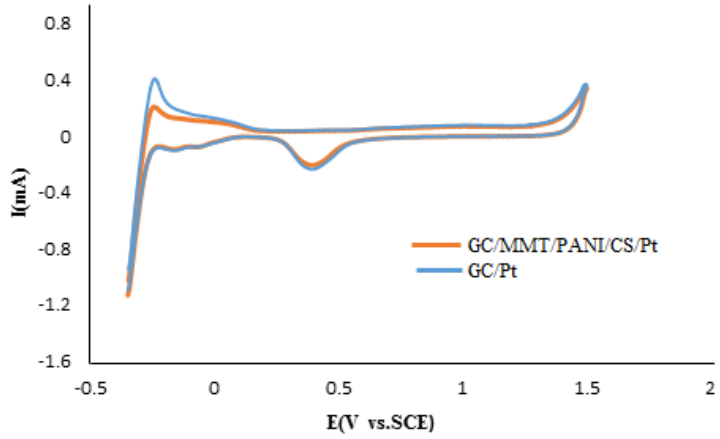

Fig. 6. Cyclic voltammograms of GC /Pt and GC/MMT/PANI/CS/Pt electrodes in 0.3 mol L^{-1} $HClO_4$ solution run at 50 mVs^{-1} at room temperature

Table 2. Physical characteristics of GC/MMT/PANI/CS/ Pt and GC/Pt as determined from the charge corresponding to the hydrogen adsorption peaks in Fig. 6

Electrode	GC/Pt	GC/MMT/PANI/CS/Pt
Pt loading (mg cm^{-2})	0.011	0.011
Q_0 (mC cm^{-2})	0.21	0.21
Q_H (mC cm^{-2})	4.14	5.14
ECSA (cm^2 mg^{-1})	1800	2235

3.4. Parameters affecting the electrooxidation of ethanol

3.4.1. Effect the amount of Pt

The anodic current of CH_3CH_2OH oxidation, depends on the amount of deposited platinum loading at the surface MMT /PANI/CS composite [23,36]. In this work, the effect of different

platinum loading ranging from 0.0058 to 0.016 mg cm^{-2} at the surface of GC/MMT/PANI/CS/Pt electrode was investigated. As is evident in Figure 7A, the current density increases with increasing the Pt loading at the surface of MMT/PANI/CS composite up to about 0.011 mg cm^{-2}. It seems that at lower Pt loading, the metal nanoparticles are almost uniformly deposited at the surface of the MMT/PANI/CS composite and the real area of the Pt nanoparticles increases which result in an enhancement in the electrocatalytic activity of the modified electrode. As shown in this Figure, at higher Pt loading, the current density remains constant and it seems that in this case, there is not any accessible surface for deposition of the Pt nanoparticles at the surface of the modified electrode.

3.4.2. Effect of MMT/PANI composite loading

Figure 7B, shows the effect of the amount of MMT/PANI composite on the anodic peak current density of the ethanol oxidation. As is seen in this Figure, the current density increases with increasing the amount of the composite up to about 0.08 w/v% and then it remains almost constant.

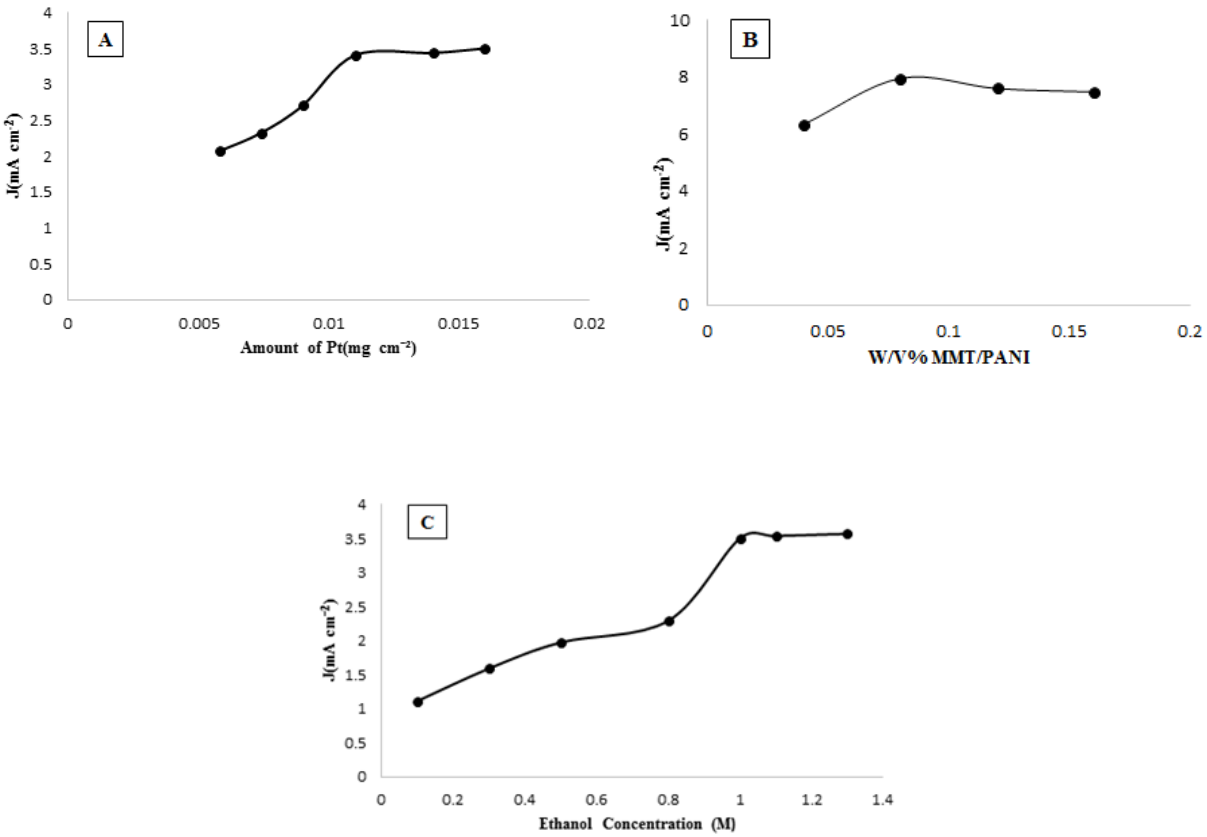

Fig. 7. Anodic peak current of (A) 1M ethanol in 0.3 M $HClO_4$ as a function of platinum loading, (B) 1M ethanol in 0.3 M $HClO_4$ solution as a function of MMT/PANI loading and (C) as a function of ethanol concentration at MMT/PANI/CS/Pt electrode in 0.3 M $HClO_4$

The increase in the peak current density may be due to the better lamination of MMT that provides a three dimensional matrix for Pt nanoparticles deposition and the occupation of the Pt nanoparticles in the pores of the MMT/PANI with the real sizes [29]. But at higher percentage, than 0.08 w/v%, the current density does not change, which seems that the active sites of the electrode surface remain constant.

3.4.3. Effect of ethanol concentration

Figure7C, shows the effect of ethanol concentration on the anodic peak current of ethanol electrooxidation. It is clearly observed that the anodic peak current density increases with increasing the ethanol concentration up to 1 M and then remains almost constant. It seems that at higher concentrations of ethanol, the active sites at the surface of the electrode are saturated. Therefore, the optimum concentration of ethanol to obtain a higher anodic peak current density may be considered as about 1 M.

3.5. Kinetic investigation

For further investigation the effect of the of MMT/PANI/CS on the electrocatalytic activity of the Pt catalyst, we carried out the Tafel studies. Figure 8, shows the typical Tafel plots for ethanol oxidation at GC/MMT/PANI/CS/Pt and GC/Pt electrodes. According to the Tafel equation [29], the values of J_0 at GC/MMT/PANI/CS/Pt and GC/Pt electrodes were calculated and they were found to be: 25 $mAcm^{-2}$ and 11 $mAcm^{-2}$, respectively. Comparison of the exchange current densities shows that the J_0 value of the GC/MMT/PANI/CS/Pt electrode is about 2.27 times higher than that of GC/Pt electrode which indicates that the electrooxidation of ethanol molecules at the GC/MMT/PANI/CS/Pt electrode is easier that of the GC/Pt electrode.

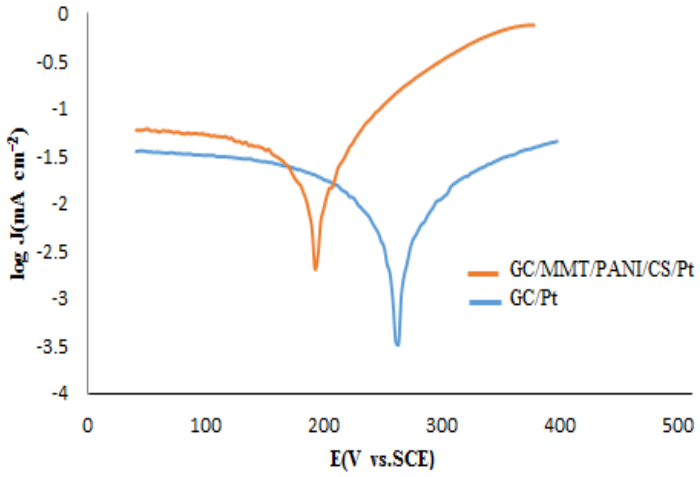

Fig. 8. Tafel plots of GC/MMT/PANI/CS/Pt and GC/Pt electrode

4. CONCLUSION

In this study, we prepared a novel MMT/PANI/CS/Pt electrocatalyst for fabrication an electrode for electrooxidation of ethanol molecules. The GC/MMT/PANI/CS/Pt constructed electrode, was characterized by scanning electron microscopy and energy dispersive X-ray spectroscopy. The electrochemical behavior of the GC/MMT/PANI/CS/Pt electrode was studied by cyclic voltammetry, electrochemical impedance spectroscopy and chronoamperometry techniques. The experimental results show that the GC/MMT/PANI/CS/Pt electrode has a much higher electrochemical activity toward the electrooxidation of ethanol molecules compared to the GC/Pt electrode. In addition, comparison of the Tafel plots shows that the GC/MMT/PANI/CS/Pt modified electrode has a higher exchange current density (J_0) than that of the GC/Pt electrode.

Acknowledgements

The authors gratefully acknowledge the support of this work by Ferdowsi University of Mashhad, Mashhad, Iran (Grant No. 3/37652)

REFERENCE

[1] F. Li, Y. Guo, M. Chen, H. Qiu, X. Sun, W. Wang, Y. Liu, and J. Gao, Int. J. Hydrogen Energy 38 (2013) 14242.
[2] R. Carrera, R. Fuentes, F. M. Cuevas, J. Ledesma, and L. G. Arriaga, J. Power Sources 269 (2014) 370.
[3] J. B. Xu, T. S. Zhao, Y. S. Li, and W. W. Yang, Int. J. Hydrogen Energy 35 (2010) 9693.
[4] Y. Zhanga, H. Shua, G. Changa, K. Ji, M. yam, X. Liua, and Y. Hea, Electrochim. Acta 109 (2013) 570.
[5] Y. Wang, S. Zou, and W. Cai, Catalysts 5 (2015) 1507.
[6] S. Meenakshi, K. G. Nishanth, P. Sridhar, and S. Pitchumani, Electrochim. Acta 135 (2014) 52.
[7] Y. H. Chu, and Y. G. Shui, Int. J. Hydrogen Energy 35 (2010) 11261.
[8] S. Shen, T. S. Zhao, J. Xu, and Y. Li, Energy Environ Sci. 4 (2011) 1428.
[9] J. Tayal, B. Rawat, and S. Basu, Int. J. Hydrogen Energy 36 (2011) 14884.
[10] S. J. Peighambardoust, S. Rowshanzamir, and M. Amjadi, Int. J. Hydrogen Energy 35 (2010) 9349.
[11] J. Tayal, B. Rawat, and S. Basu, Int. J. Hydrogen Energy 37 (2012) 4597.
[12] Y. Oh, J. Kang, S. Nam, S. Byun, and B. Park, Mater. Chem. Phys. 135 (2012) 188.
[13] Z. Jiang, Z. Jiang, and Y. Meng, Appl. Surf. Sci. 257 (2011) 2923.
[14] J. Ma, H. Sun, F. Su, Y. Chen, Y. Tang, T. Lu, and J. Zheng, Int. J. Hydrogen Energy 36 (2011) 7265.

[15] J. Barroso, A. R. Pierna, T. C. Blanco, E. Morallón, and F. Huerta, J. Power Sources 196 (2011) 4193.
[16] S. García-Rodríguez, S. Rojas, M. A. Pena, J. L. G. Fierro, S. Baranton, and J. M. Léger, Appl. Catal, B 106 (2011) 520.
[17] S. García-Rodríguez, M. A. Pena, J. L. G. Fierro, and S. Rojas, J. Power Sources 195 (2010) 5564.
[18] E. M. Cunha, J. Ribeiro, K. B. Kokoh, and A. R. de Andrade, Int. J. Hydrogen Energy 36 (2011) 11034.
[19] L. Maa, H. He, A Hsu, and R. Chen, J. Power Sources 241 (2013) 696.
[20] N. Long d, T. Hien, T. Asaka, M. Ohtaki, and M. Nogami, Int. J. Hydrogen Energy 36 (2011) 8478.
[21] L. Dong, R. R. S. Gari, Z. Li, M. M. Craig, and S. Hou, Carbon 48 (2010) 781.
[22] X. Hu, C. Lin, L. Wei, C. Hong, Y. Zhang, and N. Zhuang, Electrochim. Acta 187 (2016) 560.
[23] J. Parrondo, R. Santhanam, F. Mijangos, and B. Rambabu. Int. J. Electrochem. Sci. 5 (2010) 1342.
[24] H. Gharibi, M. Amani, H. Pahlavanzadeh, and M. Kazemeini, Electrochim. Acta 97 (2013) 216.
[25] R. Yue, Q. Zhang, C. Wang, Y. Du, P. Yang, and J. Xu, Electrochim. Acta 107 (2013) 292.
[26] S. C. Zignani, V. Baglio, J. J. Linares, G. Monforte, E. R. Gonzalez, and A. S. Arico, Int. J. Hydrogen Energy 38 (2013) 11576.
[27] H. Zhao, L. Li, J. Yang, and Y. Zhang, J. power Sources 184 (2008) 375.
[28] Z. Z. Zhu, Z. Wang, and H. L. Li, Appl. Surf. Sci. 254 (2008) 2934.
[29] E. Saghi, G. H. Rounaghi, A. Sarafraz-Yazdi, I. Razavipanah, and P. M. Moosavi, RSC Adv. 6 (2016) 113240.
[30] Y. J. Huang, Y. S. Ye, Y. J. Syu, B. J. Hwang, and F. C. Chang, J. Power Sources 208 (2010) 144.
[31] B. Ghanbarzadeh, H. Almasi, and S. A. Oleyaei, Int. J. Food Eng. 10 (2014) 121.
[32] B. Yalcin, and M. Cakmak, Polymer 45 (2004) 66238.
[33] C. H. Zhou, Appl. Clay Sci. 53 (2011) 87.
[34] M. B. Ahmad, Y. Gharayebi, M. S. Salit, M. Z. Hussein, and K. Shameli, Int. J. Mol. Sci. 12 (2011) 6040.
[35] S. Ghosh, A. L. Teillout, D. Floresyona, P. D. Oliveira, A. Hagege, and H. Remita, Int. J. Hydrogen Energy 40 (2015) 4951.
[36] C. C. Yang, T. Y. Wu, H. R. Chen, T. H. Hsieh, K. S. Ho, and C. W. Kuo, Int. J. Electrochem. Sci. 6 (2011) 1642.
[37] C. S. Choi, S. J. Park, and H. J. Choi, Curr, Appl. Phys. 7 (2007) 352.

[38] F. J. Liu, L. M. Huang, T. C. Wen, C. F. Li, S. L. Huang, and A. Gopalan, Synth. Met. 158 (2008) 603.
[39] C. N. H. Thuc, A. C. Grillet, L. Reinert, F. Ohashi, H. H. Thuc, and L. Duclaux, Appl. Clay Sci. 49 (2010) 229.
[40] P. M. Moosavi, A. R. Astaraei, A. Karimi, M. Moshiri, L. Etemad, M. Zeinali, and Gh. Karimi, Appl. Clay Sci. 103 (2015) 62.
[41] I. Razavipanah, G. H. Rounaghi, and H. Arbab-Zavvar, J. Iran. Chem. Soc. 10 (2013) 1279.
[42] L. Zhang, and F. Li, Appl. Clay Sci. 50 (2010) 64.
[43] K. Ding, Y. Zhao, L. Liu, Y. Cao, Q. Wang, H. Gu, X. Yan, and Z. Cuo, Int. J. Hydrogen Energy 39 (2014) 17622.
[44] J. B. Raoof, A. Nozad Golikand, and M. Baghayeri, J. Solid State Electrochem. 14 (2010) 817.
[45] B. Hirschorn, M. E. Orazem, B. Tribollet, V. Vivier, I. Frateur, and M. Musiani. Electrochim. Acta 55 (2010) 6218.
[46] R. Wang, T. Zhou, X. Qiu, H. Wang, Q. Wang, H. Feng, V. Linkov, and S. Ji, Int. J. Hydrogen Energy 38 (2013) 10381.